05

Effect of numerical aperture on the ultrashort laser pulses focusing in bulk of synthetic diamond

© Y.S. Gulina, J. Zhu, G.K. Krasin, E.V. Kuzmin

Lebedev Physical Institute, Russian Academy of Sciences,
119991 Moscow, Russia

e-mail: gulinays@lebedev.ru

Received December 24, 2023
Revised December 24, 2023
Accepted January 15, 2024

The effect of the focusing optics numerical aperture (NA) on the plasma channels formation induced by 1030 nm ultrashort laser pulses in bulk of synthetic diamond is investigated. It is shown that in the studied peak power range $P_0 = 0.45-0.9$ MW at $NA < 0.2$ the nonlinear focusing regime takes place, in which the significant influence of Kerr self-focusing leads to the extended plasma channels formation, and with tight focusing ($NA > 0.3$) it happens in the linear regime, where due to the predominance of geometric focusing the formation of more compact structures is possible. The transition from a nonlinear to a linear focusing depends on the power of the laser pulses and at lower powers occurs at higher values of the numerical aperture. The results obtained can be used to improve the accuracy of in-bulk laser micro/nanomodification and to control the spatial parameters of the modified regions.

Keywords: ultrashort laser pulses, nonlinear optical interaction, numerical aperture, filamentation, synthetic diamond, plasma channels, luminescence.

DOI: 10.61011/0000000000

Introduction

The study of the parameters of nonlinear optical bulk interaction of ultrashort laser pulses (USP) with crystalline dielectric materials is currently of great interest both in terms of fundamental aspects of solid state physics and for solving applied problems. The use of femtosecond laser pulses characterized by short duration and high peak intensity makes it possible to provide unprecedented precision and control for laser-induced micromodification of materials in promising and rapidly-developing areas such as the creation of functional devices for micro/nanoelectronics [1], perspective optical memory [2], diamond tracing [3,4].

During USP propagation through a dielectric material, the electric field of these pulses induces nonlinear polarization response inside the material resulting in intensity-dependent variation of the material's refraction index known as the optical Kerr effect [5]. Due to the fact that for most materials the nonlinear refraction index is positive, the refractive index in the near-axial region increases, which leads to nonlinear self-focusing of the beam [6]. On the other hand, with an increase in the intensity of laser radiation in a dielectric material, a process of photoionization occurs, leading to the formation of dense plasma and local decrease in the refractive index, resulting in beam defocusing [7]. Dynamic balance between the Kerr self-focusing and plasma defocusing results in formation of filamentation channels — extended regions with consistently high energy density [8]. The filamentation process directly affects the energy absorption efficiency and the formation of plasma channels that define the dimensions of material modification area and the rate of change.

Formation of plasma channels is affected by various factors, including laser properties (beam quality, pulse duration, wavelength, etc.), medium properties (nonlinear refraction index (n_2), linear refraction index (n_0) and multiphoton absorption factor), as well as focusing geometry. A study of the dependence of the critical power of self-focusing on the pulse duration was carried out in [9], where linearly and circularly polarized laser pulses with wavelengths of 515 and 1030 nm were focused into fused silica, fluorite, natural and synthetic diamond. The effect of laser polarization state on filamentation was assessed in [10] by the luminescence analysis of plasma channels generated in synthetic diamond produced in high pressure and high temperature (HPHT) conditions when exposed to focused USP. Formation of plasma channels is known to depend greatly on the laser beam focusing conditions [11,12]. A higher numerical aperture ensures stronger focusing resulting in higher plasma density [13,14]. Although, the effect of geometrical focusing on the Kerr self-focusing and plasma defocusing was established, a transition point where geometrical focusing dominates in the plasma channel formation process has not been identified yet. The effect of geometrical focusing on filamentation in air was studied by analyzing wavefront sags showing the optical path difference between the wavefront center and edges [15]. This method was extended to cover the analysis of filamentation in fused silica [16]. However, the role of focusing, in particular, numerical aperture (NA) of focusing optics, is still unknown and opens a wide research area, especially considering the varying plasma density in strong and weak focusing conditions.

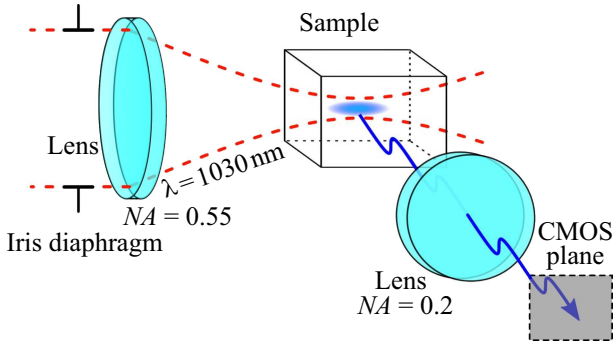

Figure 1. Experimental setup

Thus, it is important to study the focusing optics parameters, in particular, numerical aperture, on the filamentation process resulting in plasma channel formation inside the dielectric material. Synthetic diamonds produced in HPHT conditions (known for its unique thermal and optical properties, having high thermal conductivity, wide bandgap and stable optical nonlinearity) serves as an excellent platform for study of nonlinearly optical interaction between USP and propagation medium, which will further enhance the accuracy and efficiency of the femtosecond laser technology for micro/nanomodification of materials.

Experiment

The experiment was carried out on a laser setup where Satsuma optical fiber laser (Amplitude System) with fundamental wavelength 1030 nm (TEM_{00}) served as a laser light source. Ultrashort laser pulses with a duration of 300 fs, repetition rate of 100 kHz and peak power $P_0 = 0.45$ and 0.9 MW were focused inside a IIA type synthetic HPHT-diamond with dimensions $3 \times 1.5 \times 1.5$ mm (Figure 1). USP were focused into the sample by a microlens with numerical aperture $NA = 0.55$, and the numerical aperture was varied in the range $NA = 0.15{-}0.45$ using an iris diaphragm placed in front of the microlens, thus, providing the focal spot radius in the waist at $1/e^2$ within $w_0 \sim 0.73{-}2.2\,\mu$m.

Multi-pulsed USP focusing at 1030 nm provided nonlinear interband photoexcitation of free-exciton photoluminescence (PL) inside the material [10,17] with formation of extended plasma channels in the rear focal plane of the microlens. Visualization of plasma channels was performed through the side of the sample, at right angle to the laser propagation axis using a CMOS camera through the microlens with $NA = 0.2$.

Results and discussion

Microimages of USP-induced plasma channels inside the diamond sample are shown in Figure 2, and the corresponding luminescence intensity distribution sections are shown in Figure 3. At peak pulse power $P_0 = 0.45$ MW, luminescent channels occurred around the central position of the linear focus $z_f \sim 1300\,\mu$m. As the numerical aperture increased, an increase in the luminescence intensity was observed and accompanied by simultaneous decrease in channel length, while their shape remained almost symmetrical (Figure 2, *a*, 3, *a*) that may be explained by minor contribution of nonlinear effects and prevalence of geometrical linear focusing.

The effect of the Kerr and geometrical focusing on the plasma defocusing compensation was assessed in accordance with the analytical model proposed in [16]. The model is based on the analysis of the wavefront sags S that represent an optical path difference between the center and edge points of the laser beam wavefront. For Gaussian beam focusing, the sag caused by geometrical focusing is defined [18] as

$$S_G = R(z) - \sqrt{R(z)^2 - w(z)^2} \sim \frac{w_0^2}{2z_R^2}(z - f), \qquad (1)$$

where

$$R(z) = (z - f)\left(1 + \left(\frac{Z_R}{z - f}\right)\right)$$

— wavefront curvature radius,

$$w(z) = w_0\sqrt{1 + \left(\left(\frac{z - f}{z_R}\right)^2\right)}$$

— laser beam radius,

$$w_0 = \frac{\lambda}{\pi}\frac{\sqrt{(1 - NA^2)}}{NA}$$

— focal spot radius, λ — laser wavelength, $z_R = \frac{\pi w_0^2}{\lambda}$ — Rayleigh length, f — geometrical focus position.

Wavefront sags caused by the Kerr self-focusing and plasma defocusing may be obtained by finding the optical path difference between the wavefront center and edge:

$$S(z) = -\int_0^z \Delta n_{nl}(z')dz', \qquad (2)$$

where $\Delta n_{nl}(z)$ is the refraction index difference induced by the corresponding nonlinear effect.

Increase in the refraction index caused by the Kerr effect, $\Delta n_{\mathrm{Kerr}}(z) = n_2 I_0(z)$, where n_2 is the nonlinear refraction index of medium, $I_0(z) = 2P_0/\pi w(z)^2$ is the peak laser intensity, P_0 is the peak laser pulse power.

Thus, the wavefront sap from the Kerr effect may be defined [16] as

$$S_K(z) = \frac{2P_0 n_2 z_R}{\pi w_0^2}\left(\tan^{-1}\frac{z - f}{z_R} + \tan^{-1}\frac{f}{z_R}\right). \qquad (3)$$

Local decrease in the refraction index due to formation of plasma $\Delta n_{pl}(z) = -\rho(z)/2\rho_c$, where $\rho(z)$ is the plasma

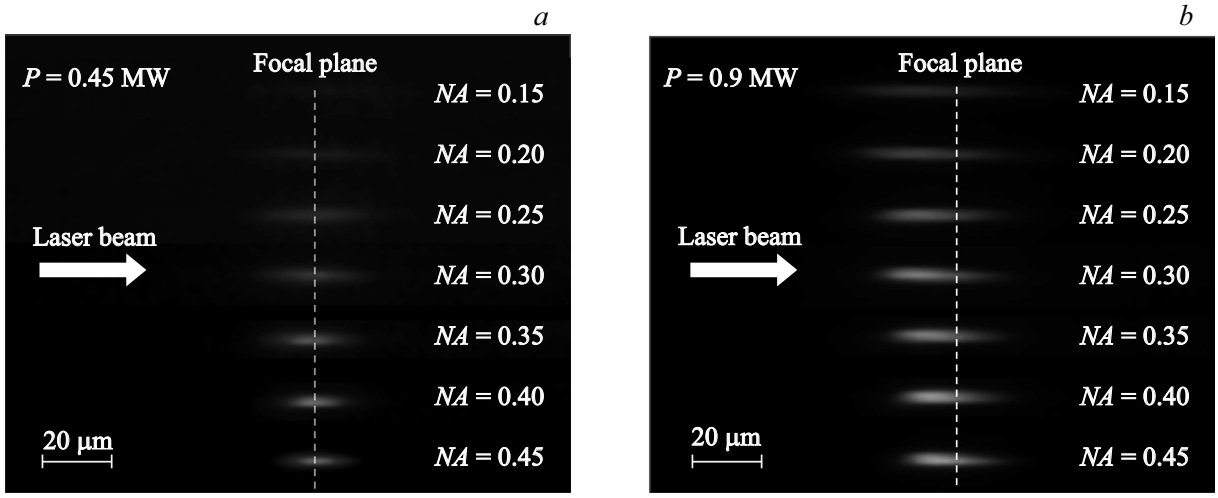

Figure 2. Microimages of USP-induced plasma channels obtained with peak power $P_0 = 0.45$ (a), 0.9 MW (b).

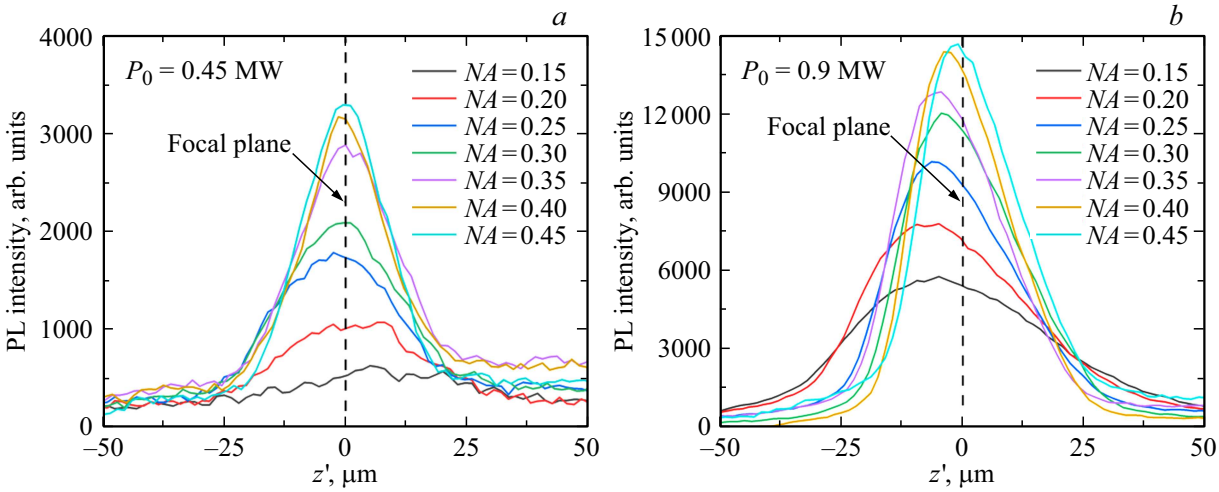

Figure 3. luminescence intensity distribution sections in plasma channels induced by USP with peak power $P_0 = 0.45$ (a), 0.9 MW (b).

density at the optical axis and $\rho_c = \omega^2 \varepsilon_0 m_e^* / e^2$ is the critical plasma density, where e is the electron charge, $m_e^* = 0.3 m_e$ is the effective electron mass [19], ω is the electromagnetic radiation frequency, ε_0 is the vacuum dielectric permittivity. Considering that the plasma density is defined by the photoionization rate, the sag caused by the plasma defocusing may be defined [16] as

$$S_P(z) = -\tau / 2\rho_c \int_0^z W_{PI}(z')dz', \qquad (4)$$

where τ is the pulse duration, W_{PI} is the photoionization rate.

Plasma density depends on the rate of seed processes such as multiphoton and tunnel ionization. The Keldysh theory [20] describing the interaction between the laser radiation and the matter serves as the fundamental for electron density growth simulation on the basis of photoionization processes. Under this theory, the multiphoton and tunnel photoionizations are set as two limiting conditions of the same physical phenomenon — ionization in the variable electromagnetic field. To define the condition of interaction between the light field and matter, the Keldysh parameter is used [21]

$$\gamma = \frac{\omega}{e} \sqrt{\frac{m_e^* c n_0 \varepsilon_0 E_g}{I_0}}, \qquad (5)$$

where n_0 is the linear refraction index of the medium, c is the speed of light in vacuum, E_g is the bandgap.

Thus, at low laser intensities, multiphoton ionization functions as the dominating process, and the Keldysh parameter $\gamma > 1.5$ [22]. The tunnel ionization takes place in extra intense laser fields at laser pulse duration < 10 fs or intensities $> 10^{14}$ W/cm^2 [23]. In our case, in the power range under study $P_0 = 0.45-0.9$ MW with weak focusing ($NA = 0.15$), the Keldysh parameter varies within $\gamma = 79-1.5$, and with strong focusing ($NA = 0.45$), it varies within $\gamma = 261-0.4$. Therefore both processes —

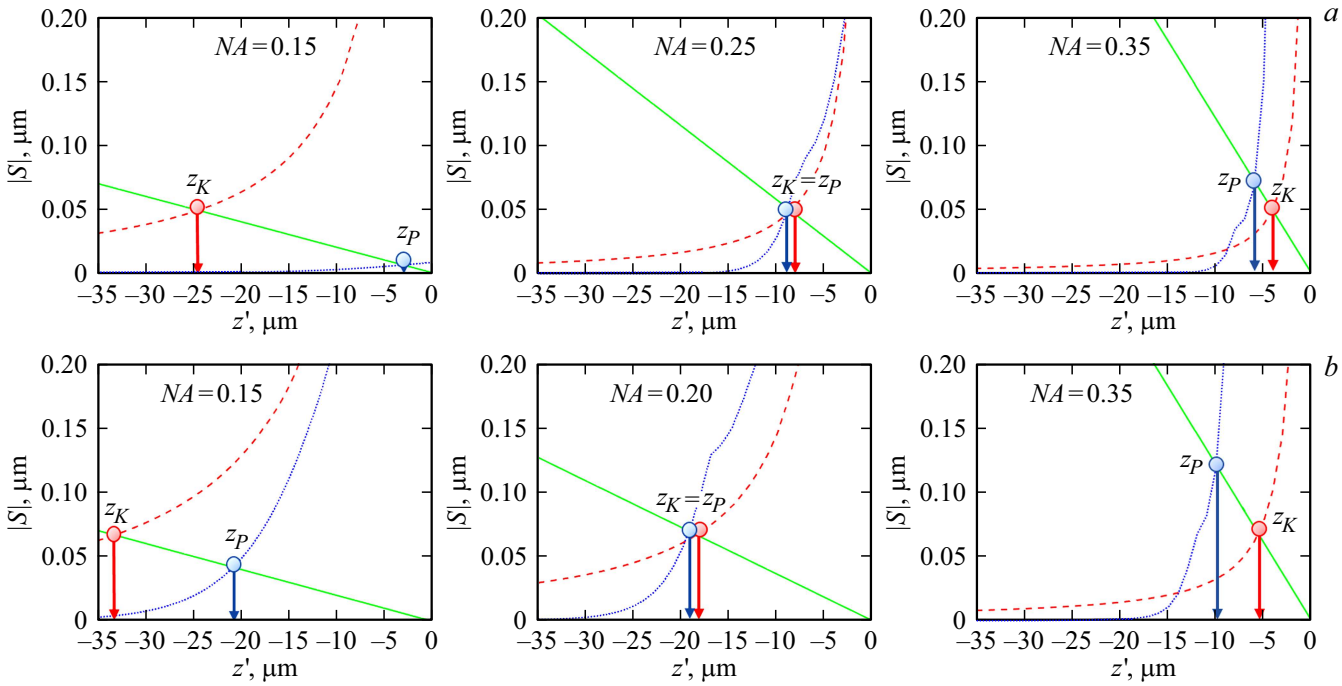

Figure 4. Dependence of the wavefront sag on the distance from the focal plane z' in various focusing conditions or peak powers $P_0 = 0.45$ (*a*), 0.9 MW (*b*): geometrical focusing — S_G, green curve; Kerr self-focusing — S_K, red curve; plasma defocusing — S_P, blue curve.

multiphoton and tunnel — make their contribution and the full photoionization rate is calculated by expression [24]

$$W_{PI} = \frac{2\omega}{9\pi}\left(\frac{\sqrt{1+\gamma^2}}{\gamma}\frac{m_e^*\omega}{\hbar}\right)^{3/2} Q\left(\gamma,\ \frac{E_g^{**}}{\hbar\omega}\right) \times \exp\left\{-\pi\left(\frac{E_g^{**}}{\hbar\omega}+1\right)\left[K\left(\frac{\gamma}{\sqrt{1+\gamma^2}}\right)-E\left(\frac{\gamma}{\sqrt{1+\gamma^2}}\right)\right] \Big/ E\left(\frac{\gamma}{\sqrt{1+\gamma^2}}\right)\right\}, \quad (6)$$

where $Q(\gamma, x)$ is the pre-exponential term described by the function

$$Q(\gamma, x) = \left[\pi/2K\left(\frac{\gamma}{\sqrt{1+\gamma^2}}\right)\right]^{1/2} \times \sum_{n=0}^{\infty}\exp\left\{-\pi\left[K\left(\frac{\gamma}{\sqrt{1+\gamma^2}}\right)-E\left(\frac{\gamma}{\sqrt{1+\gamma^2}}\right)\right] \times n/E\left(\frac{\gamma}{\sqrt{1+\gamma^2}}\right)\right\}\phi\left\{\left[\pi^2\left(2\langle x+1\rangle - 2x + n\right)/2K \times \left(\frac{\gamma}{\sqrt{1+\gamma^2}}\right)E\left(\frac{\gamma}{\sqrt{1+\gamma^2}}\right)\right]^{1/2}\right\}, \quad (7)$$

K and E is the complete elliptic integrals of the first and second kind. ϕ — is the Dawson integral defined as

$$F(x) = e^{-x^2}\int_0^x e^{-t^2}dt,$$

E_g^{**} — is the effective bandgap equal to

$$E_g^{**} = \frac{2}{\pi}E_g\frac{\sqrt{1+\gamma^2}}{\gamma}E\left(\frac{\gamma}{\sqrt{1+\gamma^2}}\right). \quad (8)$$

Graphs of the dependence of the wavefront sags on the distance from the focal plane z' in various focusing conditions for peak powers closer to the filamentation threshold power $P_0 = 0.45$ MW [14] and double threshold power $P_0 = 0.9$ MW calculated using equations (1)–(8) are shown in Figure 4, *a* and 4, *b*, respectively. It can be seen that far from the geometrical focus, the laser intensity is low and geometrical focusing (S_G — green curve) prevails over the nonlinear effects, therefore, both nonlinear effects — self-focusing and plasma defocusing are minor at a large distance from the focal plane. The contribution of the Kerr nonlinearity starts growing closer to the geometric focus and after point z_K where the sags from the Kerr (S_K — red curve) and geometrical focusing are equal to $|S_K| = |S_G|$, nonlinear self-focusing starts prevailing over the linear one, this results in nonlinear focus shift towards the laser radiation. With further approach to the focus due to an increase in intensity, plasma density starts growing resulting in beam defocusing (corresponding sap S_P — blue curve),

and after point z_P, where $|S_P| = |S_G|$, plasma defocusing prevails over the geometrical focusing. With weak focusing ($NA < 0.2$) for both powers under study, contribution of the nonlinear self-focusing starts increasing earlier than increase in the plasma density occurs ($z_P > z_K$), therefore the Kerr nonlinearity plays a dominating role, which is expressed in formation of extended plasma channels, and nonlinear focusing mode may be suggested. In strong focusing conditions ($NA > 0.3$), geometrical focusing ensures sufficient intensity for dense plasma generation and plasma defocusing starts earlier than nonlinear self-focusing is able to develop ($z_K > z_P$). This results in laser energy localization near the geometrical focus region and in formation of compact plasma channels, and then focusing continues in the linear mode. A transient mode is also observed where both self-focusing and plasma defocusing make equal contributions to the nonlinear optical interaction process: for power $P_0 = 0.45\,\mathrm{MW}$ $z_K \sim z_P$ at $NA = 0.25$, and for power $P_0 = 0.9\,\mathrm{MW}$ — at $NA = 0.2$.

For both powers under study, some general patterns may be highlighted: with increase in the numerical aperture, geometrical focusing becomes more significant, and the considerable influence of the Kerr effect takes place closer to the focal plane, while plasma defocusing, on the contrary, takes place earlier, and as the laser pulse power increases, its effect becomes more pronounced. Thus, in weak focusing conditions ($NA < 0.2$), nonlinear type of focusing is suggested, and with strong focusing ($NA > 0.3$) — linear focusing is suggested, while for apertures $NA = 0.2{-}0.25$, a transient mode is observed. The findings match well with the experimental data obtained in [14] for plasma channel photoluminescence yield with various apertures, where it has been shown that with weak focusing ($NA = 0.15,\ 0.2$), as the pumping energy increases, luminescence yield growth is little if any, and all energy is spent to increase the channel lengths, and as the pulse energy increases with strong focusing ($NA > 0.3$), monotonic luminescence yield growth of the dense plasma, localized near the focal region, is observed.

Conclusion

The studies carried out in this work on the influence of the numerical aperture of the focusing optics on the process of formation of plasma channels induced by femtosecond laser pulses inside synthetic diamond showed that in the studied range of peak powers $P_0 = 0.45{-}0.9\,\mathrm{MW}$ in weak focusing conditions ($NA < 0.2$), nonlinear type of focusing is observed (significant effect of Kerr self-focusing results in formation of extended plasma channels). With strong focusing ($NA > 0.3$) linear type of focusing is observed, which allows the formation of more compact structures. Transition from nonlinear to linear type of focusing depends on the laser pulse power, and with higher apertures takes place with lower laser powers.

Funding

The authors are grateful to the Russian Science Foundation for the financial support of these research within project 21-79-30063; https://rscf.ru/project/21-79-30063/.

Conflict of interest

The authors declare that they have no conflict of interest.

References

[1] S. Kudryashov, A. Nastulyavichus, G. Krasin, K. Khamidullin, K. Boldyrev, D. Kirilenko, A. Yachmenev, D. Ponomarev, G. Komandin, S. Lebedev, D. Prikhod'ko, M. Kovalev. Opt. Las. Technol., **158** (A), 108873 (2023). DOI: 10.1016/j.optlastec.2022.108873

[2] K. Sugioka, Y. Cheng. Light: Sci. Appl., **3** (4), 149 (2014). DOI: 10.1038/lsa.2014.30

[3] R.A. Khmelnitsky, O.E. Kovalchuk, Y.S. Gulina, A.A. Nastulyavichus, G.Y. Kriulina, N.Y. Boldyrev, S.I. Kudryashov, A.O. Levchenko, V.S. Shiryaev. Diamond and Related Materials, **128**, 109278 (2022). DOI: 10.1016/j.diamond.2022.109278

[4] Yu.S. Gulina, R.A. Khmelnitsky, O.E. Kovalchuk. Opt. i spectr., **131** (2), 247 (2023). DOI: 10.21883/OS.2023.02.55015.1-23

[5] P.L. Kelley. Phys. Rev. Lett., **16** (9), 384 (1966). DOI: 10.1103/PhysRevLett.16.384

[6] J.H. Marburger. Progr. Quant. Electron., **4** (1), 35 (1975). DOI: 10.1016/0079-6727(75)90003-8

[7] F.F. Chen. *Introduction to plasma physics and controlled fusion* (Springer International Publishing, Switzerland, 2016). DOI: 10.1007/978-3-319-22309-4

[8] A. Couairon, A. Mysyrowicz. Phys. Rep., **441** (2–4), 47 (2007). DOI: 10.1016/j.physrep.2006.12.005.

[9] S.I. Kudryashov, P.A. Danilov, E.V. Kuzmin, Y.S. Gulina, A.E. Rupasov, G.K. Krasin, I.G. Zubarev, A.O. Levchenko, M.S. Kovalev, P.P. Pakholchuk, S.A. Ostrikov, A.A. Ionin. Opt. Lett., **47** (14), 3487 (2022). DOI: 10.1364/ol.462693

[10] G.K. Krasin, Y.S. Gulina, E.V. Kuzmin, V.P. Martovitskii, S.I. Kudryashov. Photonics, **10** (2), 106 (2023). DOI: 10.3390/photonics10020106

[11] A.Q. Wu, I.H. Chowdhury, X. Xu. Appl. Phys. Lett., **88** (11), 11502 (2006). DOI: 10.1063/1.2183361

[12] E.N. Glezer, E. Mazur. Appl. Phys. Lett., **71** (7), 882 (1997). DOI: 10.1063/1.119677

[13] F. Théberge, W. Liu, P.T. Simard, A. Becker, S.L. Chin. Phys. Rev. E, **74** (3), 036406 (2006). DOI: 10.1103/PhysRevE.74.036406

[14] Y. Gulina, J. Zhu, G. Krasin, E. Kuzmin, S. Kudryashov. Photonics, **10** (10), 1177 (2023). DOI: 10.3390/photonics10101177

[15] K. Lim, M. Durand, M. Baudelet, M. Richardson. Sci. Rep., **4** (1), 7217 (2014). DOI: 10.1364/cleo_qels.2015.ftu4d.4

[16] N. Naseri, G. Dupras, L. Ramunno. Opt. Expr., **28** (18), 26977 (2020). DOI: 10.1364/OE.395185

[17] S.I. Kudryashov, P.A. Danilov, N.A. Smirnov, N.G. Stsepuro, A.E. Rupasov, R.A. Khmelnitskii, E.A. Oleynichuk, E.V. Kuzmin, A.O. Levchenko, Y.S. Gulina, S.N. Shelygina, I.V. Sozaev, M.S. Kovalev, O.E. Kovalchuk. Appl. Surf. Sci., **575**, 151736 (2022). DOI: 10.1016/j.apsusc.2021.151736

[18] L. Khan. *Laser Filamentation — Beyond Self-focusing and Plasma Defocusing* (University of Central Florida, Orlando, 2014). URL: http://purl.fcla.edu/fcla/etd/CFE0005520
[19] M. Kozák, T. Otobe, M. Zukerstein, F. Trojánek, P. Malý. Phys. Rev. B, **99**, 104305 (2019). DOI: 10.1103/PhysRevB.99.104305
[20] L.V. Keldysh. Sov. Phys. JETP, **20**, 1307 (1965).
[21] C.B. Schaffer, A. Brodeur, E. Mazur. Meas. Sci. Technol., **12**, 1784 (2001). DOI: 10.1088/0957-0233/12/11/305
[22] R. Osellame, G. Cerullo, R. Ramponi. *Femtosecond laser micromachining: photonic and microfluidic devices in transparent materials* (Springer Berlin, Heidelberg, 2012). DOI: 10.1007/978-3-642-23366-1
[23] S.S. Mao, F. Quéré, S. Guizard, X. Mao, R.E. Russo, G. Petite, P. Martin. Appl. Phys. A, **79**, 1695 (2004). DOI: 10.1007/s00339-004-2684-0
[24] C. Ferris. *Theoretical modeling of laser-induced absorption phenomena in optical materials* (University of Nebraska, Lincoln, 2014). URL: http://digitalcommons.unl.edu/elecengtheses/52

Translated by E.Ilinskaya